

# Synthesis of Macroporous Titania and Inorganic Composite Materials from Coated Colloidal Spheres—A Novel Route to Tune Pore Morphology

Dayang Wang, Rachel A. Caruso, and Frank Caruso\*

Max Planck Institute of Colloids and Interfaces, D-14424 Potsdam, Germany

Received September 27, 2000. Revised Manuscript Received November 2, 2000

A new method for fabricating macroporous inorganic and inorganic composite materials with tailored pore morphologies (i.e., pore wall thickness and open or closed pore structure) is described. Polystyrene (PS) colloidal spheres coated with polyelectrolyte (PE) multilayers (PS–PE) or silica nanoparticle (SiO<sub>2</sub>)/PE hybrid multilayers (PS–SiO<sub>2</sub>/PE) have been used as templates to produce macroporous structures. By infiltration of a titanium dioxide (TiO<sub>2</sub>) precursor, titanium (IV) isopropoxide, into templates of close-packed coated colloidal spheres, followed by removal of the organic material (PS core and PE layers) by calcination, macroporous TiO<sub>2</sub> and inorganic composite structures were produced. The pore morphology of the resulting macroporous structures depends on the nature of the multilayers deposited on the colloidal spheres. Open pore structures were obtained by templating close-packed assemblies of PS–PE colloidal spheres, while a closed pore structure was achieved by templating PS–SiO<sub>2</sub>/PE particle assemblies. The wall thickness of the resulting pores can also be tuned by altering the number of multilayers deposited on the colloidal spheres. Increasing the number of multilayers on the spheres causes an increase in the wall thickness of the macroporous structures.

## Introduction

Porous materials are of significant interest because they can possess an attractive and unique set of properties, such as high specific surface area, high damping capacity, low thermal conductivity, and low dielectric permittivity. Consequently, porous materials have a wide range of applications (both structural and functional): for example, as lightweight structural materials,<sup>1</sup> catalytic supports and surfaces,<sup>2</sup> thermal and acoustic insulators,<sup>3</sup> optical devices,<sup>4</sup> and candidates for high-speed computer device packaging.<sup>5</sup> According to their pore sizes, porous materials can be classified into three types: microporous, mesoporous, and macroporous. Microporous materials are characterized by pore sizes of  $\leq 2$  nm. Pores are in the range of 2–50 nm for mesoporous structures, and those of macroporous materials are generally regarded as being  $> 50$  nm in diameter.<sup>6</sup>

Fabrication pathways for microporous and mesoporous structures are well established.<sup>7</sup> Their synthesis

is typically achieved by using templating molecules that are removed after the formation of the desired structures. Microporous materials (e.g., zeolites) are usually templated by organic amine molecules,<sup>8</sup> while surfactant or block copolymer assemblies are generally used as the templating species for mesoporous materials.<sup>9</sup>

Recently, macroporous materials with well-defined and controllable porosity have attracted interest because of their unique optical, catalytic, and mechanical properties. For example, macroporous supports could be designed to provide optimal flow and improved efficiencies in catalysis and large molecule separation processes as well as to permit immobilization and stabilization of large guest molecules, including biological molecules.<sup>10</sup>

A number of different strategies have been utilized to produce macroporous materials.<sup>1,4,10–21</sup> Decomposi-

(7) Ozin, G. A. *Adv. Mater.* **1992**, *4*, 612.

(8) Bein, T. *Chem. Mater.* **1996**, *8*, 1636.

(9) (a) Kramer, E.; Forster, S.; Goltner, C.; Antonietti, M. *Langmuir* **1998**, *14*, 2027. (b) Zhao, D. Y.; Yang, P. D.; Huo, Q. S.; Chmelka, B. F.; Stucky, G. D. *Curr. Opin. Solid State Mater. Sci.* **1998**, *3*, 111. (c) Goltner, C.; Antonietti, M. *Adv. Mater.* **1997**, *9*, 431.

(10) Seshadri, R.; Meldrum, F. C. *Adv. Mater.* **2000**, *12*, 1149.

(11) Androff, N. W.; Francis, L. F.; Velamakanni, B. V. *AICHE J.* **1997**, *43*, 2878.

(12) Lange, F. F.; Miller, K. T. *Adv. Ceram. Mater.* **1987**, *2*, 827.

(13) Verwell, H.; Dewith, G.; Veeneman, D. *J. Mater. Sci.* **1985**, *20*, 1069.

(14) Melosh, N. A.; Lipic, P.; Bates, F. S.; Wudl, F.; Stucky, G. D.; Fredrickson, G. H.; Chemelka, B. F. *Macromolecules* **1999**, *32*, 4332.

(15) Walsh, D.; Mann, S. *Nature* **1995**, *377*, 320.

(16) Walsh, D.; Hopwood, J. D.; Mann, S. *Science* **1994**, *264*, 1576.

(17) Imhof, A.; Pine, D. J. *Nature* **1997**, *389*, 948.

(18) Kiefer, J.; Hilborn, J. G.; Hedrick, J. L. *Polymer* **1996**, *37*, 5715.

(19) Xia, Y.; Gates, B.; Yin, Y.; Liu, Y. *Adv. Mater.* **2000**, *12*, 693.

(20) Velev, O. D.; Kaler, E. W. *Adv. Mater.* **2000**, *12*, 531.

(21) Holland, B. T.; Blanford, C. F.; Do, T.; Stein, A. *Chem. Mater.* **1999**, *11*, 795.

\* To whom correspondence should be addressed. Fax: +49 331 567 9202. E-mail: frank.caruso@mpikg-golm.mpg.de.

(1) Wu, M.; Fujii, T.; Messing, G. L. *J. Non-Cryst. Solids* **1990**, *121*, 407.

(2) Harold, M. P.; Lee, C.; Burggraaf, A. J.; Keizer, K.; Zaspalis, V. T.; de Lange, R. S. A. *Mater. Res. Soc. Bull.* **1994**, *19*, 34.

(3) Litovsky, E.; Shapiro, M.; Shavit, A. *J. Am. Ceram. Soc.* **1996**, *79*, 1366.

(4) (a) Subramania, G.; Constant, K.; Biswas, R.; Sigalas, M. M.; Ho, K. M. *Appl. Phys. Lett.* **1999**, *74*, 3933. (b) Holland, B. T.; Blanford, C. F.; Stein, A. *Science* **1998**, *281*, 538. (c) Wijnhoven, J. E. G. J.; Vos, W. L. *Science* **1998**, *281*, 802.

(5) Miller, R. D. *Science* **1999**, *286*, 421.

(6) (a) Schaefer, D. W. *Mater. Res. Soc. Bull.* **1994**, *19*, 14. (b) Langley, P. J.; Hulliger, J. *Chem. Soc. Rev.* **1999**, *28*, 279.

tion of foam agents,<sup>11</sup> replication of polymer foams,<sup>12</sup> and foaming of sol-gel solutions<sup>1</sup> are well-known processing methods for macroporous ceramics, an important branch of lightweight materials. These methods often produce materials with irregular pore shapes, large pores (generally  $>10\ \mu\text{m}$ ), and broad pore size distributions. Templating techniques similar to those used for the fabrication of micro- or mesoporous materials (i.e., using surfactants or block copolymers<sup>7,9</sup>) have also been employed to successfully produce macroporous materials.<sup>14</sup> Recently, the skeletons of organisms such as echinoids (sea urchins) have been used to template the formation of macroporous materials with pore sizes in the micrometer range.<sup>10</sup>

The method of emulsion templating is perhaps one of the most general and has been employed to produce macroporous calcium carbonate,<sup>15</sup> calcium phosphate,<sup>16</sup> titania, silica, and zirconia with pore sizes ranging from 50 nm to several micrometers.<sup>17</sup> Highly monodisperse emulsion droplets and hence pores can be obtained in a controlled manner. As the volume fraction of the inner phase exceeds the highest packing density of spheres (74%), the inner phase will be interconnected. This is known as a high internal phase emulsion. If the phase surrounding an emulsion is solidified, for example, by using polymerization for organic materials or sol-gel chemistry for inorganic materials, a macroporous structure is obtained upon removal of the inner phase, which is usually a low molecular weight liquid such as water.<sup>18</sup> The resulting macroporous structure is considered as a replica of the inner phase, with interconnected pores, otherwise referred to as an open pore structure. Conversely, in closed pore structures, the pores are not interconnected by "channels" but are "closed" individual voids in the matrix.

An alternative and promising approach to the fabrication of macroporous materials with open pore structure is the use of colloidal assemblies as templates.<sup>4,19-21</sup> Monodisperse polystyrene or silica spheres can self-assemble into an ordered three-dimensional (3D) array. The ordered arrays offer a 3D scaffold in which a variety of precursors can be infiltrated. After subsequent solidification of the precursors and removal of the colloidal spheres, macroporous structures are obtained. Such 3D structures that are comprised of highly ordered air spheres interconnected to each other by small channels are known as inverse opals.<sup>19-21</sup> The dimension of the pores depends on the diameters of the colloidal spheres. Because well-known techniques exist for producing colloidal spheres with various diameters, pore sizes can be varied easily. The major advantage of this method is that it provides a simple and effective route to the fabrication of macroporous materials with controlled pore sizes and well-defined periodic structures.<sup>4</sup>

Numerous properties of macroporous materials, such as density, thermal conductivity, and dielectric permittivity, are mainly dependent on their pore morphology (e.g., pore size, wall thickness, and structure).<sup>1,4,10-21</sup> Porous materials with different pore morphologies have varied applications: for example, an interconnected open pore structure, as is the case for inverse opals,<sup>19-21</sup> is critical to the formation of a true photonic band gap,<sup>1</sup> while low dielectric materials usually require closed pore structures.<sup>5</sup> The pore wall thickness is another

important parameter because it generally determines mechanical stability of the final products.

Templating techniques using colloidal assemblies have in the past suffered from a number of limitations for tailoring the pore morphology of macroporous materials. Fine control of pore wall thickness and the formation of structures with closed pores have been difficult to achieve. In the case of emulsion templating procedures, closed pores can be achieved, but only when the volume fraction of the inner phase is lower than 30%, which leads to a decrease in total porosity.<sup>18</sup> Imhof and Pine prepared closed pore TiO<sub>2</sub> foams by using nonaqueous emulsions as templates in which the water phase was replaced by another liquid, yielding a broad distribution of pore sizes.<sup>22</sup> Recently, some control of the pore wall thickness was obtained by diluting precursors or by appropriate thermal treatment upon template removal.<sup>21</sup> To our knowledge, colloidal assemblies of commonly used particles such as SiO<sub>2</sub> and polystyrene have not been previously used as templates for the formation of closed-pore macroporous materials.

Micrometer-sized polystyrene spheres coated with PE or silica nanoparticle/PE multilayers are fabricated by the layer-by-layer assembly<sup>23</sup> of oppositely charged polyelectrolytes or polyelectrolyte and silica nanoparticles, respectively, onto colloidal templates.<sup>24,25</sup> This approach provides a facile way to form core-shell structures with exquisite control over wall thickness, composition, and size. (The thickness of the shell can be readily controlled by varying the number of coating cycles.) Herein, we report a novel templating route based on colloidal assemblies of *coated* colloid particles for the fabrication of macroporous materials with tailored pore morphologies. The coated colloids can be assembled into macroscopic close-packed structures, as was recently shown for polystyrene spheres coated with zeolite nanoparticles.<sup>26</sup> In this work, we have used colloidal assemblies made from polyelectrolyte and nanoparticle/polyelectrolyte multilayer-coated spheres as templates for the formation of macroporous TiO<sub>2</sub> and inorganic composite materials. Structures with tailored pore morphologies were obtained by infiltration of a titanium dioxide precursor into the colloidal assemblies, followed by hydrolysis and subsequent calcination.

## Experimental Section

**Materials.** Poly(allylamine hydrochloride) (PAH),  $M_w = 8\ 000-11\ 000$ , poly(diallyldimethylammonium chloride) (PDAD-MAC),  $M_w < 200\ 000$ , and poly(sodium 4-styrenesulfonate) (PSS),  $M_w = 70\ 000$ , were obtained from Aldrich. PSS was dialyzed against Milli-Q water ( $M_w$  cutoff 14 000) and lyophilized before use. The SiO<sub>2</sub> nanoparticles (40 wt % SiO<sub>2</sub> suspension, Ludox TM 40, diameter of  $26 \pm 4$  nm) were purchased from DuPont. Negatively charged sulfate-stabilized polystyrene (PS) spheres of diameter 640 nm were prepared as described elsewhere.<sup>27</sup> Sodium chloride (NaCl), 2-propanol

(22) Imhof, A.; Pine, D. J. *Adv. Mater.* **1999**, *11*, 311.

(23) Decher, G. *Science* **1997**, *277*, 1232.

(24) Caruso, F. *Chem. Eur. J.* **2000**, *6*, 413.

(25) (a) Donath, E.; Sukhorukov, G. B.; Caruso, F.; Davis, S. A.; Möhwald, H. *Angew. Chem., Int. Ed.* **1998**, *37*, 2201. (b) Caruso, F.; Caruso, R.; Möhwald, H. *Science* **1998**, *282*, 1111. (c) Caruso, F.; Möhwald, H. *J. Am. Chem. Soc.* **1999**, *121*, 6039.

(26) Rhodes, K. H.; Davis, S. A.; Caruso, F.; Zhang, B.; Mann, S. *Chem. Mater.* **2000**, *12*, 2832.

(27) Furusawa, K.; Norde, W.; Lyklema, J. *Kolloid-Z. Z. Polym.* **1972**, *250*, 908.

(IPA), and titanium(IV) isopropoxide (TIP) were purchased from Aldrich. The water in all experiments was prepared in a three-stage Millipore Milli-Q Plus 185 purification system and had a resistivity higher than 18.2 M $\Omega$  cm.

**Coating of PS Spheres with PE Multilayers (PS-PE).** 1 mL of a 0.5 mg mL<sup>-1</sup> PAH solution containing 0.5 M NaCl was added to 0.2 mL of negatively charged PS spheres ( $\approx 10^{10}$  spheres). The dispersion was occasionally stirred, and a period of 20 min was allowed for PAH adsorption. The dispersion was then centrifuged at 10 000g for 15 min, the supernatant was removed,  $\approx 2$  mL of water was added, and the spheres were redispersed with gentle shaking. The coated particles were washed by three alternate centrifugation/resuspension cycles. This ensured removal of free PAH from solution. Using the same procedure and conditions, a polyanion layer was deposited by subsequent adsorption of PSS (1 mL of 1 mg mL<sup>-1</sup>/0.5 M NaCl) onto the PAH-coated spheres. The desired number of PAH/PSS multilayers was assembled by the repeated consecutive coating of PAH and PSS. In this work, PS spheres coated with either a 5-layer PE film [(PAH/PSS)<sub>2</sub>/PAH] (PS-PE<sub>5</sub>) or a 21-layer PE film [(PAH/PSS)<sub>10</sub>/PAH] (PS-PE<sub>21</sub>) were used as templates for the fabrication of macroporous TiO<sub>2</sub> structures.

**Coating of PS Spheres with SiO<sub>2</sub>/PE Multilayers (PS-SiO<sub>2</sub>/PE).** Prior to the deposition of the SiO<sub>2</sub>/PDADMAC hybrid layer, the "primer" three-layer PE film, PDADMAC/PSS/PDADMAC, was coated on the PS spheres (as described above). The outer PDADMAC layer made the coated particles positively charged. A SiO<sub>2</sub>/PDADMAC hybrid layer was fabricated by adding 0.5 mL of the aqueous SiO<sub>2</sub> suspension to the PE-coated PS spheres ( $\approx 10^{10}$  spheres dispersed in 1 mL of 0.1 M NaCl), allowing 15 min for SiO<sub>2</sub> adsorption, removing excess SiO<sub>2</sub> by four repeated centrifugation (13 500g, 15 min)/water wash/redispersion cycles, and subsequently depositing PDADMAC (1 mL of 1 mg mL<sup>-1</sup> solution containing 0.5 M NaCl, adsorption time of 20 min) following the procedure outlined above.

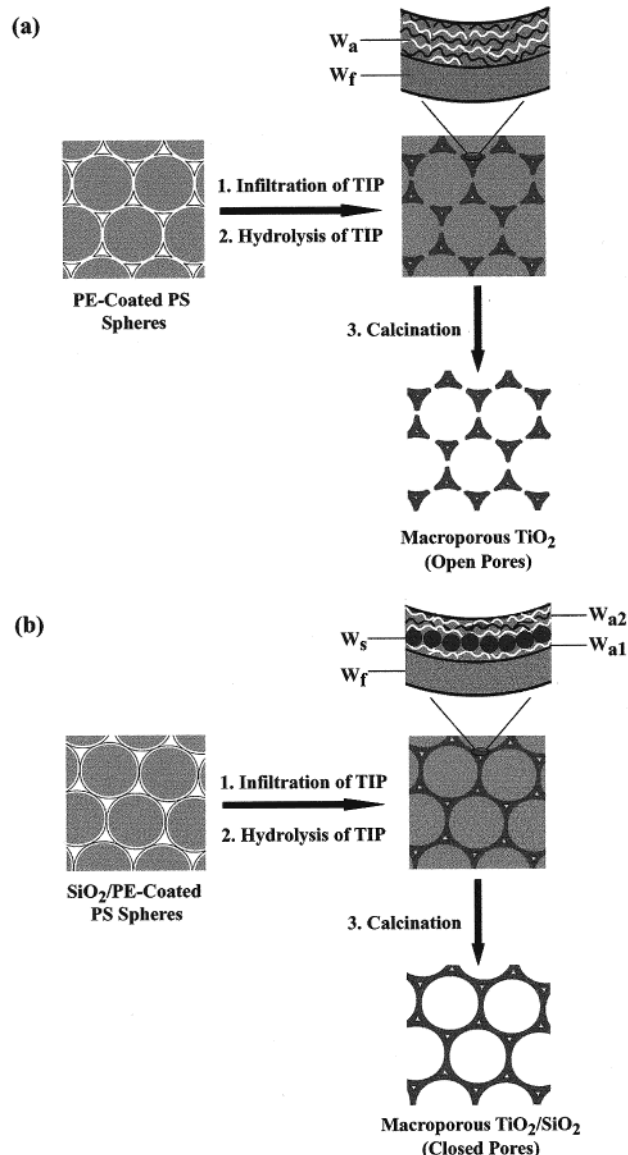
**Macroporous TiO<sub>2</sub> and TiO<sub>2</sub>/SiO<sub>2</sub> Material Fabrication.** The uncoated or coated PS spheres were centrifuged (10 min at 10 000g for PS, PS-PE<sub>5</sub>, and PS-PE<sub>21</sub>, and 13 500g for PS-SiO<sub>2</sub>/PE) to obtain sediments at the bottom of the Eppendorf tubes. After drying under ambient conditions, millimeter-sized pieces, which were used directly as templates, were obtained. The templates were placed in a 1-mL Eppendorf tube with a centrifugal filter (membrane pore size 0.1  $\mu$ m) (Millipore, USA) and wetted with 0.5 mL of IPA for 10 min. After removal of IPA by centrifugation (5000g, 10 min), a 0.5 mL of TIP/IPA solution (volume ratio of TIP to IPA of 1:1) was added to wet the templates for 10 min. Following removal of the TIP solution by centrifugation (5000g, 10 min), the samples were again dried under ambient conditions. This soaking and drying cycle was repeated five times to ensure that the voids between colloidal spheres in the templates were sufficiently filled. The PS spheres and PE layers were subsequently removed by calcination. The samples were first slowly heated to 500 °C (5 °C min<sup>-1</sup>) and then heated at 500 °C for 1–2 h under oxygen. The fabrication procedure of macroporous TiO<sub>2</sub> (anatase) structures and inorganic composites is shown in Scheme 1.

**Characterization.** Scanning electron microscopy (SEM) measurements were performed with a HITACHI S-4000-FEG instrument operated at 5 kV. SEM samples were placed on carbon surfaces and then sputter-coated with Au ( $\approx 5$ -nm thick). Transmission electron microscopy (TEM) measurements and energy-dispersive X-ray (EDX) spectra were obtained with a Philips CM12 microscope operating at 120 kV. Ultrathin sections of the macroporous TiO<sub>2</sub> samples for TEM were sliced with a Leica ultracut UCT ultramicrotome after setting them in LR-white resin. The thin sections were placed onto either carbon- or uncoated copper grids.

## Results and Discussion

### Macroporous TiO<sub>2</sub> Materials Produced from Bare and PE Multilayer-Coated PS Spheres. The

### Scheme 1. Illustration of the Procedure Used To Fabricate Macroporous (a) TiO<sub>2</sub> and (b) TiO<sub>2</sub>/SiO<sub>2</sub> Materials from Coated Colloidal Spheres<sup>a</sup>



<sup>a</sup> The scheme is not intended to convey the actual order of the structures. A schematic representation of the wall structure and pore morphology is also shown. (a)  $w_f$  represents the TiO<sub>2</sub> layer thickness of the coating at the interstitial voids between spheres and  $w_a$  the TiO<sub>2</sub> layer thickness resulting from hydrolysis of TIP adsorbed within the PE layers. It is assumed that  $w_a$  is the same as the thickness of the PE multilayers on the coated colloids. (b)  $w_{a1}$  and  $w_{a2}$  are the TiO<sub>2</sub> layer thicknesses resulting from hydrolysis of TIP absorbed by the outer PDADMAC and the primer layers, respectively.  $w_s$  corresponds to the thickness of the SiO<sub>2</sub> nanoparticle layer.

interstitial voids between the close-packed pure PS spheres can be filled with TIP solution, which can be hydrolyzed, and after removal of the PS spheres by calcination, a macroporous TiO<sub>2</sub> structure comprised of TiO<sub>2</sub> nanoparticles is formed.<sup>21</sup> Figure 1 shows SEM micrographs of the macroporous TiO<sub>2</sub> produced when using bare PS colloidal spheres of 640-nm diameter as templates. The average diameter of the pores in this macroporous structure is  $384 \pm 24$  nm and the average wall thickness of the pores is  $16 \pm 2$  nm. (Here, the pore wall thickness refers to half the total wall thickness

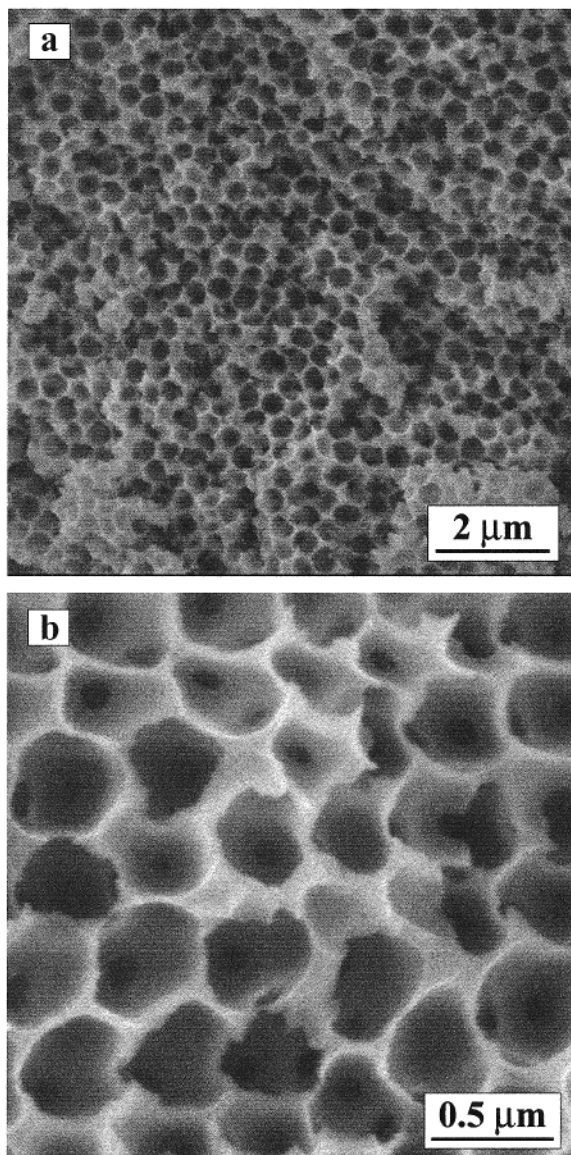


**Figure 1.** (a) Low- and (b) high-magnification SEM micrographs of the macroporous TiO<sub>2</sub> structure fabricated by templating pure PS colloidal spheres of diameter 640 nm.

between pores, that is, the wall thickness of a single pore). The center-to-center average distance between the pores is  $414 \pm 16$  nm, which corresponds to a linear shrinkage of 35% when compared to the original size of the colloidal templates (640 nm). Usually, the hydrolysis reaction of alkoxides to produce the metal oxide results in the production of large amounts of water and alcohol, leading to a small fraction of the oxide materials. Removal of the water and alcohol during drying and heat treatment contributes to a large shrinkage and cracking of the materials.<sup>28</sup> Such shrinkage and cracking of our materials was seen by SEM. At higher magnification (Figure 1b), round channels in the pore walls are clearly visible and confirm that the macropores in the resulting structure are interconnected with each other (i.e., an open pore structure is formed).

In the case of the core-shell colloidal spheres, the shell thickness is dependent on the dimensions of the

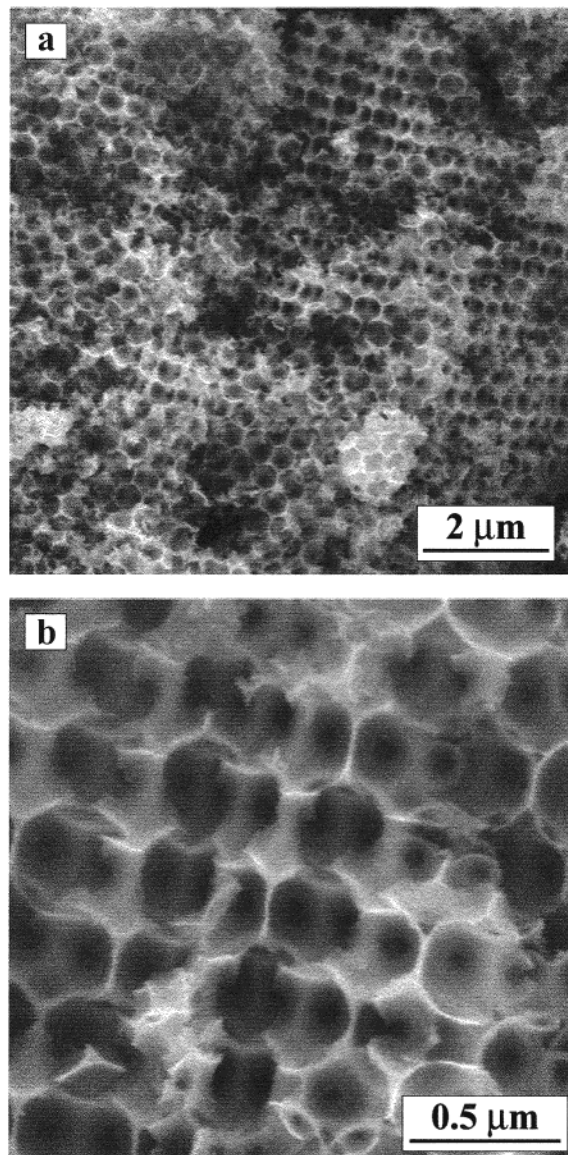


**Figure 2.** (a) Low- and (b) high-magnification SEM micrographs of the macroporous TiO<sub>2</sub> structure produced by templating PS-PE<sub>5</sub> colloidal spheres. (The diameter of the coated particles is 651 nm.<sup>29</sup>)

deposited species and the number of the deposited multilayers.<sup>24</sup> For the PS-PE<sub>5</sub> spheres, 5 PE layers, (PAH/PSS)<sub>2</sub>/PAH, were deposited on the PS particles. The thickness of the multilayer is about 6 nm and the diameter of the core-shell spheres is  $\approx 651$  nm.<sup>29</sup> With PS-PE<sub>5</sub> spheres as templates, the resulting macroporous TiO<sub>2</sub> structure possesses pores with an average size of  $421 \pm 28$  nm (Figure 2). The average center-to-center distance between the pores is  $451 \pm 20$  nm and corresponds to a shrinkage of 31%. The average wall thickness of the resulting pores is  $13 \pm 2$  nm. The SEM micrograph at higher magnification (Figure 2b) shows channels connecting the pores, which demonstrates that this resulting porous material also has an open pore structure. For the PS-PE<sub>21</sub> spheres, 21 PE layers, (PAH/PSS)<sub>10</sub>/PAH, were deposited on PS particles, yielding a diameter of 708 nm for the coated spheres

(28) Subramanian, G.; Manoharan, V. N.; Throne, J. D.; Pine, D. *J. Adv. Mater.* **1999**, *11*, 1261.

(29) Caruso, F.; Lichtenfeld, H.; Donath, E.; Möhwald, H. *Macromolecules* **1999**, *32*, 2317.

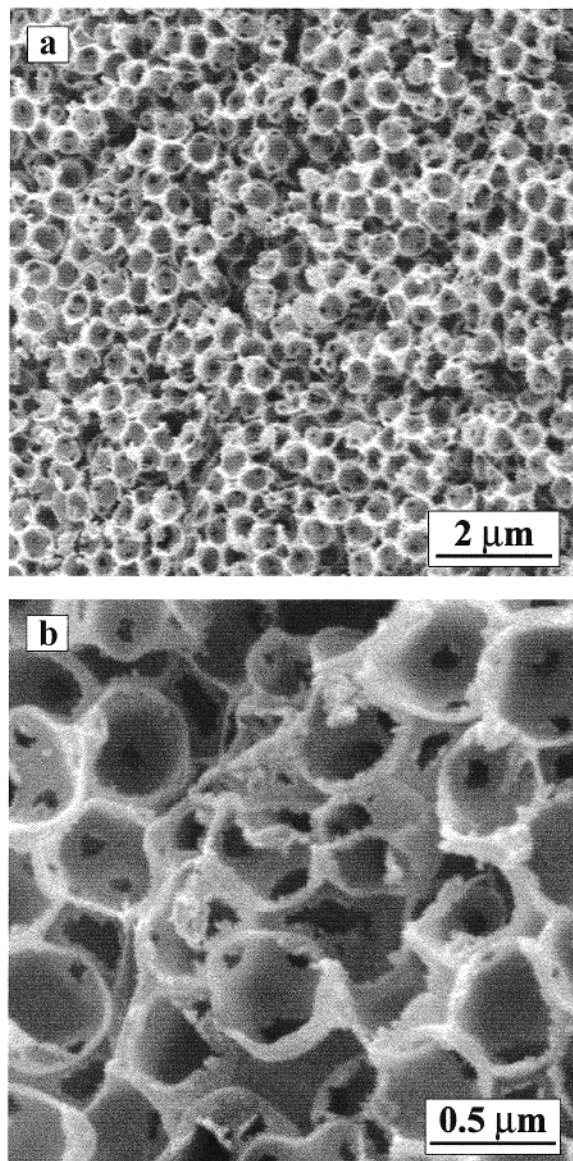


**Figure 3.** (a) Low- and (b) high-magnification SEM micrographs of the macroporous  $\text{TiO}_2$  structure fabricated by templating PS-PE<sub>21</sub> colloidal spheres. (The diameter of the coated particles is 708 nm.<sup>29</sup>)

with a multilayer shell 34-nm thick.<sup>29</sup> Figure 3 shows SEM micrographs of the macroporous  $\text{TiO}_2$  structure formed by using the PS-PE<sub>21</sub> spheres as templates. The average diameter of the pores in the resulting macroporous  $\text{TiO}_2$  structure is  $430 \pm 29$  nm and the average center-to-center distance between the pores is  $510 \pm 37$  nm, reflecting a shrinkage of 28%. The average wall thickness of the pores is  $42 \pm 7$  nm. Similar to the macroporous  $\text{TiO}_2$  structure obtained by templating PS-PE<sub>5</sub> colloidal spheres, the material resulting from the PS-PE<sub>21</sub> spheres has an open structure as the pores are interconnected by channels (Figure 3b).

When using pure PS colloidal spheres as templates, the macroporous  $\text{TiO}_2$  structure is formed via hydrolysis of the TIP in the interstitial voids between the colloidal spheres and subsequent removal of the templates. The wall thickness is dependent on the crystallization kinetics of the metal alkoxide precursors and their interaction with the colloidal spheres.<sup>4b</sup> It has been demonstrated that, on flat surfaces, PE layers can absorb metal

**Table 1. Parameters of Macroporous  $\text{TiO}_2$  and  $\text{TiO}_2/\text{SiO}_2$  Structures Formed by Using Different Colloidal Templates**

template	pore diameter (nm)	pore wall thickness <sup>a</sup> ( $w_a + w_f$ ) (nm)	center-to-center distance (nm)	shrinkage (%)	pore structure
PS	$384 \pm 24$	$16 \pm 2$ (0 + 16)	$414 \pm 16$	35	open
PS-PE <sub>5</sub>	$421 \pm 28$	$13 \pm 2$ (6 + 7)	$451 \pm 20$	31	open
PS-PE <sub>21</sub>	$430 \pm 29$	$42 \pm 7$ (34 + 8)	$510 \pm 37$	28	open
PS-SiO <sub>2</sub> /PE <sup>b</sup>	$494 \pm 22$	$33 \pm 9$ (27 + 6)	$567 \pm 18$	20	closed

<sup>a</sup> The pore wall thickness refers to half of the total wall thickness between pores. <sup>b</sup> Corresponds to PS spheres coated with three polyelectrolyte primer layers, followed by a  $\text{SiO}_2$  nanoparticle layer and an outermost PE layer (see text for details).

alkoxide solution to form composite sol-gel thin films.<sup>30</sup> Subsequent calcination results in a metal oxide thin film, the thickness of which is dependent on that of the charged polymer layers (dendrimers) and the conditions of film formation.<sup>30</sup> Therefore, in the process of infiltration of TIP into the close-packed PE-coated PS spheres, not only does TIP solution fill in the interstitial voids between the coated spheres, but it can also penetrate into the PE multilayer. Thus, the resulting macroporous  $\text{TiO}_2$  structure is formed by hydrolysis of TIP both in the interstitial voids between the spheres and within the PE multilayers. Hence, when PE-coated PS colloidal spheres are templated, the pore walls of the macroporous  $\text{TiO}_2$  material can be divided into two components: one which is due to hydrolysis of TIP filling the interstitial voids between spheres ( $w_f$ ) and the other due to hydrolysis of the TIP absorbed within the PE layers ( $w_a$ ) (see Scheme 1a). By assuming that  $w_a$  is the same as the thickness of the PE multilayers,  $w_f$  values for the resulting macroporous  $\text{TiO}_2$  structure formed by using uncoated or coated PS colloidal spheres as templates were calculated. These values are presented in Table 1. Because the same TIP crystallization kinetics (for example, the same TIP concentration and hydrolysis conditions), were employed and because the outermost PE layer of both PS-PE<sub>5</sub> and PS-PE<sub>21</sub> spheres is PAH (that is, the interaction between TIP and the surface of the PE-coated PS spheres is similar), the macroporous structures formed by templating PS-PE<sub>5</sub> or PS-PE<sub>21</sub> colloidal spheres would be expected to have similar  $w_f$  values. The data indeed reveal that macroporous  $\text{TiO}_2$  structures templated by PS-PE<sub>5</sub> and PS-PE<sub>21</sub> spheres have similar  $w_f$  values, 7 and 8 nm, respectively. In comparison to the 16-nm wall thickness of the macroporous  $\text{TiO}_2$  structure formed by templating pure PS colloidal spheres, the difference in  $w_f$  values is most likely due to the differences in the interaction between TIP and the positively charged PAH compared with that between TIP and the negatively charged sulfate groups on the bare PS spheres. Table 1 implies that increasing the thickness of the PE multilayers causes an increase in  $w_a$  for the macroporous  $\text{TiO}_2$  structure, which is responsible for the increase of the total wall thickness. This provides a means to control the wall thickness of the resulting macroporous structure.

(30) Fan, H.; Zhou, Y.; Lopez, P. *Adv. Mater.* **1997**, *9*, 728.

Although the PE multilayer can absorb the titania precursor solution, and hence formation of  $\text{TiO}_2$  can occur within the layers, the macroporous  $\text{TiO}_2$  structures templated by PE multilayer-coated PS spheres possess an open pore structure. This phenomenon could be attributed to the possibility that the TIP solution may only partially infiltrate the close-packed PE-coated sphere templates at the contact points between spheres. As a result after hydrolysis of TIP, a continuous network of  $\text{TiO}_2$  may not be formed in this part of the film. Therefore, the resulting  $\text{TiO}_2/\text{PE}$  composite films at the contact points between spheres may possess less mechanical stability compared with that of the noncontacting areas of the sphere surface. In the calcination process, this decreased stability would lead to breakage, resulting in channels forming in these walls (i.e., open pore structure). Figure 2b shows that there are round channels in the pore walls of the macroporous  $\text{TiO}_2$  structure templated by PS-PE<sub>5</sub>. These channels are similar to those of the macroporous  $\text{TiO}_2$  structure formed when templating pure PS spheres (Figure 1b). However, in the macroporous  $\text{TiO}_2$  structure formed when templating PS-PE<sub>21</sub> spheres (Figure 3b), there are irregularly shaped channels in the pore walls. This suggests that increasing the number of PE multilayers surrounding the PS spheres could increase the amount of TIP absorbed by the PE film at the contact points between spheres and hence increase the mechanical stability of the resulting  $\text{TiO}_2/\text{PE}$  composite between the spheres. With further increasing of the number of PE multilayers, macroporous  $\text{TiO}_2$  structures with closed pore structures may be possible.

#### Macroporous $\text{TiO}_2/\text{SiO}_2$ Materials Produced from $\text{SiO}_2/\text{PE}$ Multilayer-Coated PS Colloidal Spheres.

To form a uniform  $\text{SiO}_2$  nanoparticle coating on the PS particles, a 3.3 nm-thick three-layer PE film (primer layer), PDADMAC/PSS/PDADMAC, was first deposited on the PS spheres.<sup>25b</sup> Following this, a 24 nm-thick  $\text{SiO}_2$  nanoparticle/PDADMAC bilayer was deposited.<sup>25b</sup> SEM micrographs of the macroporous structures formed by templating the PS- $\text{SiO}_2/\text{PE}$  spheres show that the spheres have coalesced and few cracks on the spheres are observed (Figure 4a). The SEM micrograph of a cross section of the resulting macroporous structure demonstrates the hollow nature of the resulting spheres (Figure 4b). The macroporous material possesses a closed pore structure; that is, the interconnected pore structure obtained with PS or PE-coated PS spheres is not observed (Figure 4c). The TEM micrograph of a cross section of the macroporous  $\text{TiO}_2/\text{SiO}_2$  structure also reveals that the pores are closed (Figure 5a). At higher magnification (Figure 5b), two different types of particles with diameters of about 3 and 25 nm can be distinguished in the wall of the resulting macroporous material. An EDX spectrum (Figure 5c) obtained from this area shows peaks of Si, Ti, and O, which suggests the wall is formed from  $\text{SiO}_2$  and  $\text{TiO}_2$  particles. The smaller particles are  $\text{TiO}_2$  and the  $\approx 25$ -nm particles are  $\text{SiO}_2$ . The latter value is in agreement with the diameter of the  $\text{SiO}_2$  nanoparticles used. The average diameter of the closed pores of the macroporous  $\text{TiO}_2/\text{SiO}_2$  structure is  $494 \pm 22$  nm and the average center-to-center distance between the pores is  $567 \pm 18$  nm, corresponding to a shrinkage of 20%. It has been demonstrated

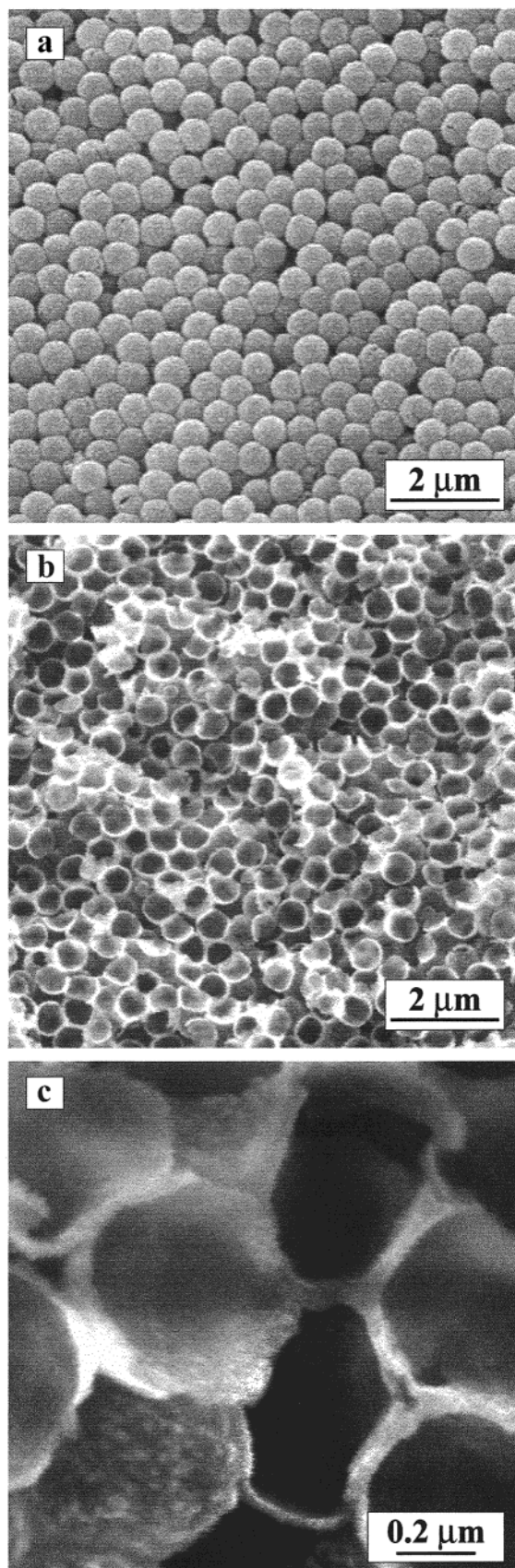


**Figure 4.** SEM micrographs of the macroporous  $\text{TiO}_2/\text{SiO}_2$  structure fabricated by templating PS- $\text{SiO}_2/\text{PE}$  colloidal spheres with a 640-nm PS core: (a) low-magnification image; (b) low- and (c) high-magnification images of cross sections. The PS spheres were coated with three polyelectrolyte primer layers, followed by a  $\text{SiO}_2$  nanoparticle layer and an outermost PE layer. (The diameter of the coated particles is 695 nm.<sup>25b,29</sup>)

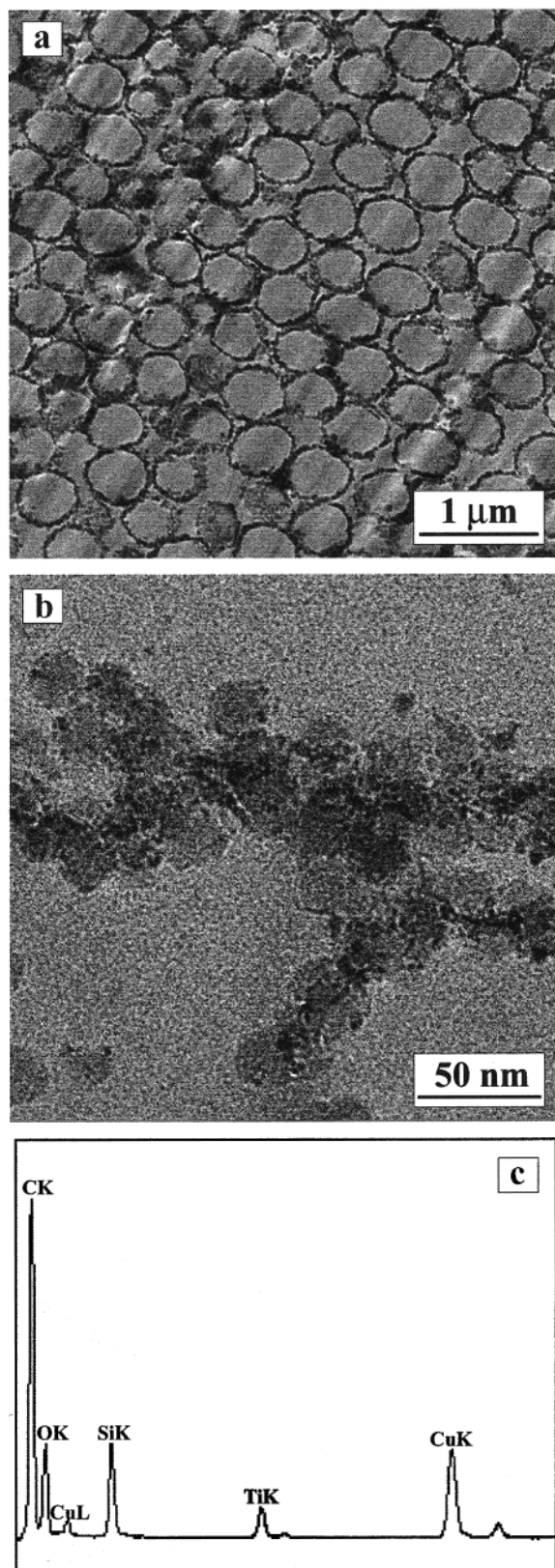


**Figure 5.** (a) Low- and (b) high-magnification TEM micrographs of cross sections and (c) EDX spectrum of the macroporous  $\text{TiO}_2/\text{SiO}_2$  structure fabricated by templating PS- $\text{SiO}_2/\text{PE}$  colloidal spheres.

that coalescence of the  $\text{SiO}_2$  nanoparticles (as a result of sintering) occurs predominantly within the individual  $\text{SiO}_2$  nanoparticle-coated PS spheres, rather than between the coated spheres.<sup>25b</sup> Coalescence of the  $\text{SiO}_2$

nanoparticles on the coated PS spheres due to the calcination process provides the structural integrity for the closed pore structures.<sup>25b</sup> Hence, the closed pore structure is attributed to the fact that the PS spheres were coated by a uniform inorganic nanoparticle layer before templating.

The average wall thickness of the  $\text{SiO}_2/\text{TiO}_2$  composite pores is  $33 \pm 9$  nm (Figures 4b and 5a). The wall thickness of the resulting pores can be divided into four parts (see Scheme 1b):  $w_f$  resulting from the hydrolysis of TIP filled in the interstitial voids between the colloidal spheres (as before),  $w_{a1}$  from hydrolysis of TIP absorbed by the outer PDADMAC layer,  $w_{a2}$  from hydrolysis of TIP absorbed by the primer layer, and  $w_s$  due to the actual thickness of the  $\text{SiO}_2$  nanoparticle layer. It is difficult to distinguish  $w_{a1}$  and  $w_{a2}$  from  $w_s$  because of the small amount of TIP absorbed by the PE layers and because the  $\text{SiO}_2$  nanoparticle layer has a large specific surface and a relatively rough surface. The  $\text{TiO}_2$  particles could be adsorbed on the  $\text{SiO}_2$  nanoparticles. If the total thickness ( $w_a$ ) of  $w_{a1}$ ,  $w_{a2}$ , and  $w_s$  is assumed to be the same as the average thickness of the  $\text{PE}_3/\text{SiO}_2/\text{PDADMAC}$  multilayer, that is, 27 nm, the  $w_f$  value of the resulting pore wall is 6 nm (after subtraction of  $w_a$  from the wall thickness, shown in Table 1). This is similar to the  $w_f$  value of the macroporous  $\text{TiO}_2$  structure formed by templating PE-coated PS colloidal spheres and can be explained by the fact that the outer layer in all three cases (PS- $\text{PE}_5$ , PS- $\text{PE}_{21}$ , or PS- $\text{SiO}_2/\text{PE}$ ) is positively charged and that the same concentration and hydrolysis conditions of TIP were used throughout. By using PS spheres coated with thicker  $\text{SiO}_2$  nanoparticle/PE multilayers<sup>25b</sup> in the templating process, the total wall thickness could be altered.

In the current work we used  $\text{SiO}_2$  nanoparticle-coated PS colloidal spheres as templates to demonstrate the ability to fabricate closed pore structure macroporous materials. Recently, we have assembled other metal oxide nanoparticles (such as zeolite,  $\text{TiO}_2$ , Laponite, and  $\text{Fe}_3\text{O}_4$ ) onto colloidal spheres by the layer-by-layer procedure and these were subsequently used to form inorganic and inorganic-organic composite hollow spheres.<sup>26,31,32</sup> These colloidal spheres coated with inorganic materials could be used as templates to produce homogeneous and heterogeneous closed pore macroporous materials suitable for a variety of technological applications, including lightweight and low dielectric materials and catalysts. These are the subjects of further investigations. The growth of colloidal crystals with coated colloidal spheres for fabricating highly ordered macroporous materials is also underway.

## Conclusion

Macroporous  $\text{TiO}_2$  and  $\text{TiO}_2/\text{SiO}_2$  materials have been prepared by using assemblies of close-packed coated colloidal spheres as templates, infiltrating titanium(IV) isopropoxide into the close-packed spheres and thereafter removing the colloidal cores and polyelectrolytes by calcination. The present work provides a new approach to fabricate inorganic macroporous materials

(31) Caruso, F.; Susha, A.; Spasova, M.; Giersig, M.; Caruso, R. A. *Chem. Mater.* **2001**, in press.

(32) Caruso, R. A.; Susha, A.; Caruso, F. *Chem. Mater.* **2001**, in press.

with tailored pore morphologies and composition. The wall thickness of the resulting macroporous materials increases with the number of PE multilayers deposited onto the colloidal spheres. The pore structure depends on the composition of the multilayer deposited on the colloidal spheres: an open pore structure can be formed by using colloidal spheres coated with PE multilayers (up to 21 layers) as templates and a closed pore structure by using colloidal spheres coated with SiO<sub>2</sub> nanoparticle and PE hybrid multilayers. We are currently preparing different macroporous inorganic materials by using colloidal spheres coated with a variety of PE multilayers and inorganic nanoparticles as tem-

plates, with the aim of introducing different properties and functionality to the final macroporous materials.

**Acknowledgment.** We thank Dangsheng Su and Gisela Weinberg (Fritz-Haber-Institute, Berlin) for assistance with SEM, Michael Giersig and Uli Blöck (Hahn-Meitner-Institute, Berlin) for help with TEM, Rona Pitschke for ultramicrotoming, and Christine Pilz for dialysis of the PSS. This work was supported by the German Federal Ministry of Education, Science, Research and Technology and the Volkswagen Foundation.

CM001184J